van Rooijen, Erik; Lotsari, Eliisa

The spatiotemporal distribution of river bank erosion events and their drivers in seasonally frozen regions

Published in:
Geomorphology

DOI:
10.1016/j.geomorph.2024.109140

Published: 01/06/2024

Document Version
Publisher's PDF, also known as Version of record

Please cite the original version:
van Rooijen, E., & Lotsari, E. (2024). The spatiotemporal distribution of river bank erosion events and their drivers in seasonally frozen regions. *Geomorphology*, *454*, Article 109140.
https://doi.org/10.1016/j.geomorph.2024.109140

Geomorphology 454 (2024) 109140

Contents lists available at ScienceDirect

Geomorphology

journal homepage: www.journals.elsevier.com/geomorphology

The spatiotemporal distribution of river bank erosion events and their drivers in seasonally frozen regions

Erik van Rooijen *, Eliisa Lotsari

Water and Environmental Engineering, Department of built environment, Aalto University, P.O. Box 15200, Tietotie 1, 00076 Aalto, Finland

A R T I C L E I N F O

Keywords:
River bank erosion
Distribution
Reindeer
Freeze-thaw

A B S T R A C T

River bank erosion supplies sediments to river systems, sustaining many river functions. To properly understand and ultimately model river bank erosion, we have to know the temporal and spatial distributions at which it occurs. This is especially challenging in cold-climate regions where a large variety of processes occur that contribute to river bank erosion. We therefore obtained a one-year dataset, using buried soil sensors, on bank erosion and its forcing parameters with a high temporal resolution to answer the question: what are the temporal and spatial distributions of river bank erosion in cold climate regions and what are the forcing conditions causing these distributions? We measured soil movements at multiple river bank sites throughout Finland and compared the movement times with soil moisture, soil and air temperature and discharge information. This analysis showed that there is no clear temporal distribution of bank movement in the Southernmost investigated site, while in the more Northern field sites soil movement was most frequent around the freezing and thawing periods. At one field site an additional period with an increased frequency of soil movement events is likely caused by reindeer during summer months. This research used a new type of dataset of soil temperature, moisture and movement. This unique dataset allowed us to identify individual soil movement events and helps to better understand river bank erosion and by extension fluvial systems in cold-climates.

1. Introduction

Rivers change shape and evolve. Processes like sedimentation and erosion cause these changes, which can have profound impacts on flood risk (Nones, 2019), shipping (e.g Frings et al., 2014; Paarlberg et al., 2015), lotic habitats (e.g. van Rooijen et al., 2022), landform changes (e.g. Asahi et al., 2013), among others. Sedimentation and erosion are intrinsically linked to the sediment supply to the river (Fuller and Marden, 2010; Rachelly et al., 2021). Changes in the amount or timing of sediment supplied to rivers can thus have major impacts on river management and fluvial ecosystem services (Fuller and Marden, 2010). Significant amounts of sediments supplied to rivers originate from river banks (Kronvang et al., 1997; Sekely et al., 2002; Neal and Anders, 2015), which therefore warrants scientific investigation into river bank erosion.

River banks form the transition between terrestrial and fluvial environments, where processes of both environments can dominate. Which processes dominate can vary both spatially as well as temporally and information on both is needed for modelling and understanding bank erosion (Lawler, 2005, 2008). As such, many different erosional processes occur and must be understood. The most well-known of these are mass failure and fluvial entrainment. Mass failure occurs when the strength of the bank changes, often due to changing pore pressures or undercutting of the bank, such that it becomes unstable. A large wedge of soil then slides or falls down the slope (Osman and Thorne, 1988; Rinaldi and Casagli, 1999; Darby et al., 2007). Fluvial entrainment occurs when the hydraulic forces on the particles of the bank are strong enough to dislodge them, and therefore always occurs below or close to the water surface (Osman and Thorne, 1988; Rinaldi et al., 2004; Darby et al., 2007; Duró et al., 2020). The required force to transport loose soil is lower than that of packed soil and soil that slid down the bank to the bank toe is transported away more rapidly than soil from the bank toe itself (Prosser et al., 2000).

Besides these processes which usually occur rapidly, also slow processes are of importance. These are generally subaerial processes, which have traditionally been considered to only be preparatory, but it has been shown they can also directly cause erosion (Prosser et al., 2000; Couper and Maddock, 2001). For example, seepage can dislodge

* Corresponding author.
E-mail address: erik.vanrooijen@aalto.fi (E. van Rooijen).

https://doi.org/10.1016/j.geomorph.2024.109140
Received 20 December 2023; Received in revised form 7 March 2024; Accepted 7 March 2024
Available online 11 March 2024
0169-555X/

particles and wash them away, slowly eroding the bank (Hagerty, 1991; Fox et al., 2007). Finally, drying can lead to desiccation cracks, weakening the soil and/or dislodging particles (Gardiner, 1983; Prosser et al., 2000).

Besides the previously mentioned bank erosion processes which can occur everywhere, several are unique to cold climate regions. For example, in these regions ice floes can remove bank material when it collides with the bank (Chassiot et al., 2020; Vandermause et al., 2021). Arguably more important the freezing and thawing of soil. When temperatures are cold enough, the soil freezes up to a certain depth. Water is sucked to this depth and an ice lens can develop, heaving the soil above (Gatto, 1995). This can make particles or sections of soil become less firmly attached, making other processes occur more readily (Gardiner, 1983; Gatto, 1995; Kimiaghalam et al., 2015), or it can cause some particles to be moved immediately upon thawing (Gatto, 1995). Finally, in these regions, border ice can develop, which can protect the bank from erosion, making any of the erosion mechanism types less likely to occur (Chassiot et al., 2020). Besides the additional processes that can occur in cold climate regions, these regions are also of interest due to the disproportionally large influence climate change has on these regions (Rasmus et al., 2020; IPCC, 2022), which will change the prevalence of these processes in the future.

The erosion processes depend on the bank composition, river flow, temperature and soil moisture, which all impact both separately and jointly to bank erosion rates. Furthermore, vegetation also impacts bank erosion, generally by their roots reinforcing the soil, reducing erosion (e.g. Easson and Yarbrough, 2002; Hubble et al., 2010). All these can change in space, and with the exception of bank composition can change in short time spans and can therefore cause both spatial and temporal variability in river bank erosion. River flow, temperature and soil moisture are considered the forcing parameters of river bank erosion as they influence the timing of erosion, and therefore the understanding of river bank erosion and its processes also requires the measurement or determination of these parameters (Couper and Maddock, 2001).

River bank erosion is complex, with many different processes and mechanisms depending on multiple forcing parameters working in tandem and varying both spatially and temporally (e.g. Lawler, 1986). This is especially true in cold climate regions where the complexity is even larger. Data showing the temporal distribution of bank erosion and its forcing parameters at a wide range of environmental conditions in cold climate regions, could thus be highly beneficial. However, until recently a long running dataset of bank erosion measurements with a high temporal resolution, measuring both the erosion and its forcing parameters directly were very demanding. In this work we will obtain such a dataset and with it aim to answer the question: what are the temporal and spatial distributions of river bank erosion in cold climate

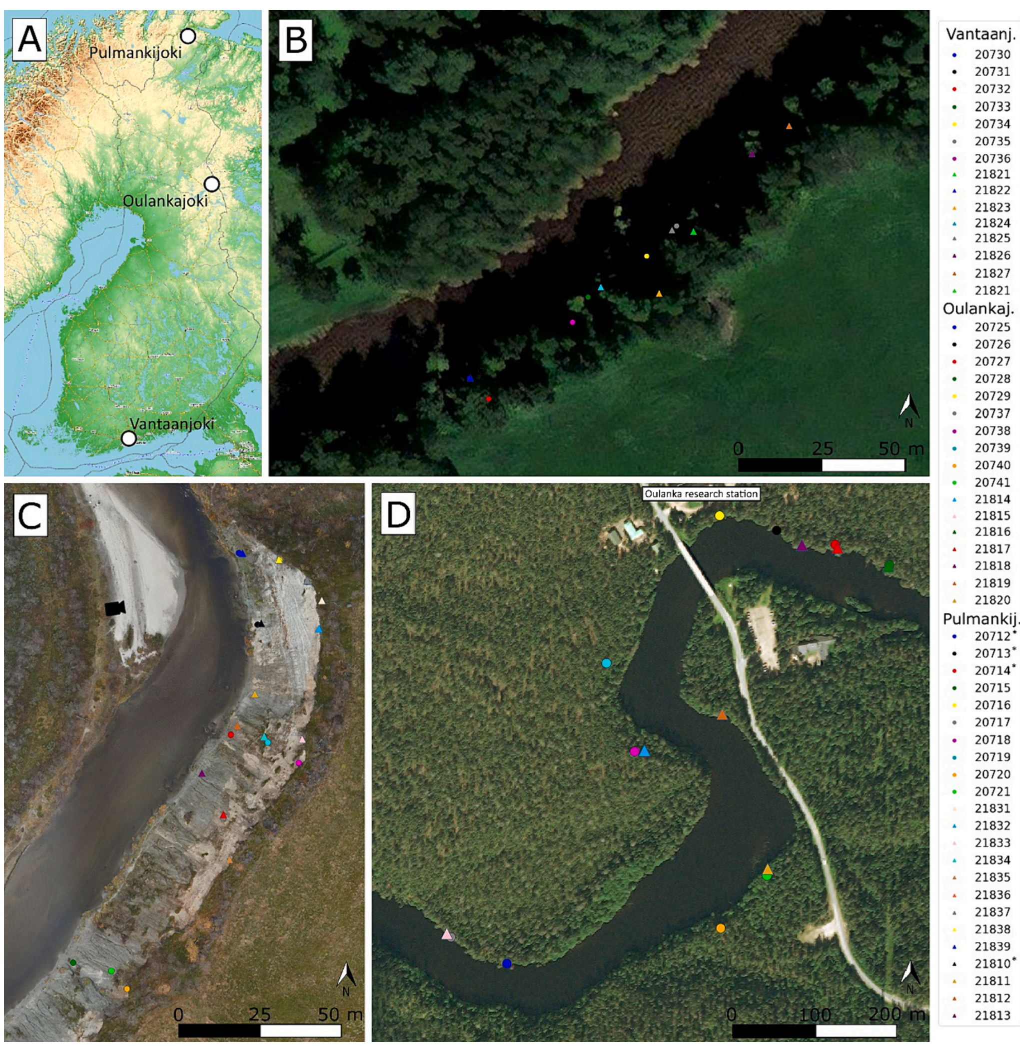

Fig. 1. Overview of the investigated fieldsites. A. locations of the fieldsites, **B**. overview of the Vantaanjoki River fieldsite, **C**. overview of the Pulmankijoki River fieldsite, including the location of the time-lapse camera and **D**. overview of the Oulankajoki River fieldsite, including the location of the Oulanka research station. The colored circles and triangles indicate the locations of installed sensors (with their ID numbers, which we refer to in this paper). Sensors with an asterisk have been lost.

regions and what are the forcing conditions causing these distributions?

2. Materials and methods

2.1. Description of field sites

The study focusses on three river reaches in Finland at the Vantaanjoki, Oulankajoki and Pulmankijoki Rivers. Despite them having different geographical, climatological and landscape settings (Fig. 1) due to their different latitudes, they all represent geomorphological characteristics and soils of FennoScandinavia due to the last deglaciation in the area (Panin et al., 2020). Further, they are representative to the wider Boreal-Arctic region in their hydro-climatic conditions. More precisely, they represent different extremes of the cold climate category of the Köppen-Geiger classification (Fig. 2), updated by Peel et al. (2007), and stages of defrosting (ice cover ~3–7 months). All of these rivers have large seasonal hydro-climatic variations, subzero winter air temperatures, maximum discharges during the spring snow-melt and erodible channels, and are projected to experience warmer winters. A short site specific description of all three sites is presented here, but more information on each site is given by van Rooijen et al. (2023).

The 200 m long Vantaanjoki bank site (Fig. 1B) is located at the southern edge of the cold climate region, and was therefore selected due to its warmer hydro-climatic conditions, and shortest ice-covered season. It is located approximately 2.5 km from Helsinki-Vantaa airport in an agricultural area close to the Helsinki metropolitan area. The sensors are located in the bank directly next to the river channel. The bank is strongly vegetated and has a mild slope (approximately 22°). The river is straight with strong anthropogenic influences. The D_{50} grain size of the bank is smaller than 0.1 mm, and therefore represents banks with cohesive materials (typical to regions under glacial lakes [Panin et al., 2020]) and vegetation within southern parts of cold climate region.

The Oulankajoki is the most continental one of the three study sites within the selected cold climate region study sites. The studied bank site covers a 1350 m long meandering reach close to the Kiutaköngäs meteorological station in the North-East of Finland in the strongly vegetated Oulanka National Park in an area with an uneven, undulating, hilly topography with slopes up to 40° and up to 70 m high (Fig. 1D). The soil consists of a shallow layer of top soil (<10 cm) on top of moraine. At the downstream part of the site, groundwater flow is present. The site belongs to reindeer management area of Finland. The grain size distribution of the bank is bimodal, with peaks around 0.25 mm and larger than 8 mm, and therefore represents banks with moraine soil and vegetation within continental parts of cold climate region. Moraine (i.e. till) is one of the most common soil types in the formerly deglaciated area.

The last bank site is in the far north of Finland along the well-studied meandering Pulmankijoki (e.g. Mansikkaniemi and Mäki, 1990; Lotsari et al., 2014, 2019; Fig. 1C), is approximately 300 m long, 18 m high and has a slope of approximately 36°, close to the friction angle of the soil material. The bank top is part of the fluvial terrace (Mansikkaniemi and Mäki, 1990). The top 1.5 m of the bank consists of loose sand, which lies on top of 15 m of laminated fine sandy silt and clayey silt (Lotsari et al., 2020). The soil is bare with only occasional tufts of grass, while shrubs and alpine birch are present on top of the bank (Lotsari et al., 2014). Footprints and photographic evidence indicate that reindeer occasionally visit the site. The site belongs to reindeer management area of Finland. The D_{50} grain size of the bank is on average 0.3 mm, and therefore represents banks with sand sized glacio-fluvial sediments (Lotsari et al., 2020) and vegetation within sub-arctic parts of cold climate region (Saarinen et al., 2013).

2.2. Sensors and dataset

Multiple soil scouts, soil monitoring devices that monitor in real-time with a 20-min sampling frequency (Tiusanen, 2013), with integrated temperature, soil moisture and inclination sensors were installed at all three sites. The sensors accuracies are 0.1 °C, 2 % and 0.004 g for temperature, soil moisture and inclination, respectively (Soil Scout, 2022). At Vantaanjoki, Oulankajoki and Pulmankioki River sites, seven, ten and ten sensors were installed, respectively, by digging a hole 10–20 cm deep and placing the sensor horizontally into the hole and then filling the hole back in. The first sets of sensors, based on which the study by van Rooijen et al. (2023) was done, were installed in May–July 2022, depending on the site. For more information on the used sensors and installation procedure see van Rooijen et al. (2023). Furthermore, an additional eight, seven and thirteen sensors were installed on 16/11/2022, 09/11/2022 and 08/11/2022 at the Vantaanjoki, Oulankajoki

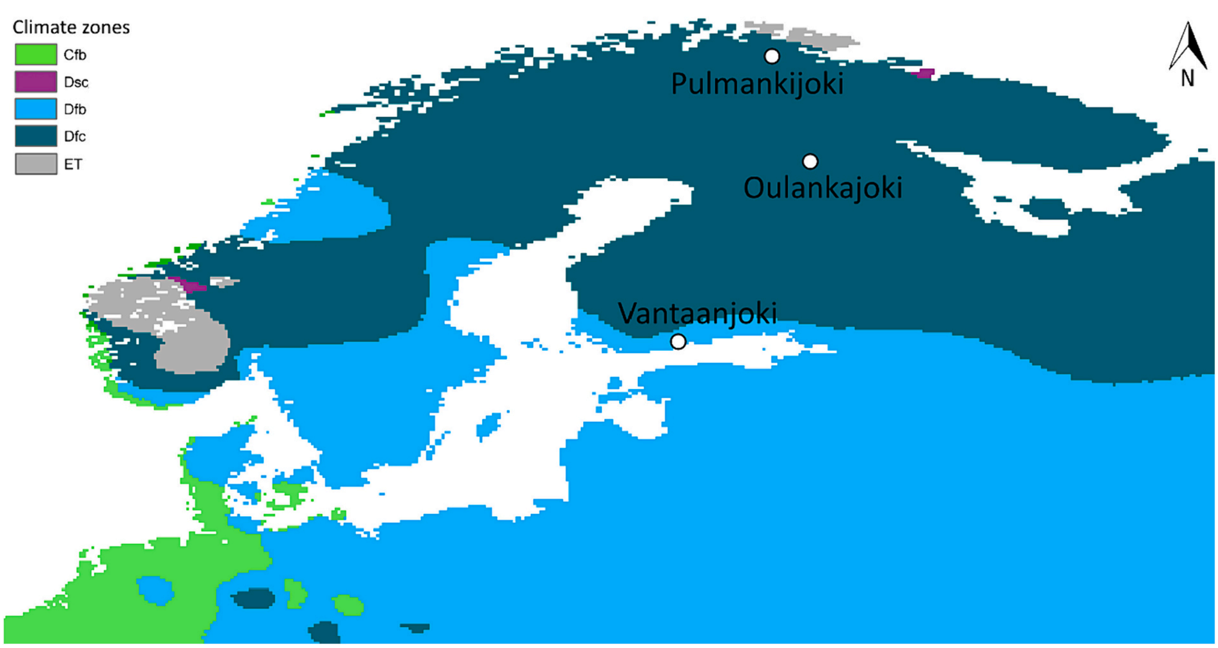

Fig. 2. Overview of the climates in Fennoscandinavia according to the Köppen-Geiger classification. The locations of the field sites of this study are also shown. Adapted from Peel et al. (2007).

and Pulmankijoki sites, respectively, due to technical issues with the previously installed sensors which resulted in soil moisture data to not be gathered. Thus, in total 15, 17 and 23 sensors were installed at the Vantaanjoki, Oulankajoki and Pulmankijoki sites, respectively (Fig. 1).

Using these sensors, a one-year dataset (starting on 17/11/2022) was obtained, containing soil moisture, soil temperature and sensor orientation with a high temporal resolution. This period covered the freezing period of late autumn 2022, snow-covered winter, thawing during spring, open-channel flow conditions of summer and following autumn, and freezing period of late autumn 2023. Soil movement can be identified from sensor orientation: the moment sensor orientation changes, soil around the sensor moves.

Discharge or water level data was used to identify floods. At the Vantaanjoki field site, the discharge measurements from the Myllymäki observation station of Finnish Environment Institute (Syke), located <1 km downstream from the field site, were used (obtained from Waterinfo, 2023). At the Oulankajoki site, discharge measurements were obtained from national observation station of Syke, which is located right next to the Oulanka Research Station of University of Oulu (obtained from Waterinfo (2023)). At the Pulmankijoki field site, no national observation station exsist, and Levelogger (Solinst) sensors were used to measure water pressure, and simultaneous air pressure data (Barologger), to obtain water depth information approximately 1.5 km downstream from the field site until 27 September 2023.

Finally, at the Pulmankijoki field site a time-lapse camera was located, observing the downstream end of the river bank, taking one photo every two hours. These photos were used as reference measurements.

2.3. Event detection algorithm

van Rooijen et al. (2023) found that soil movement in the investigated river banks is usually episodic in nature. Soil movement as measured with these sensors can broadly be categorized in three groups. The first are visible as sudden changes in inclination around at least one axis, although generally around multiple. These can be associated with mass wasting or other sudden erosional events. The second are slow continuous movements, such as creep, identifiable by prolonged unidirectional changes in inclinations around all axes (also found by van Rooijen et al., 2023 in a Palsa mire). Lastly, slow movements especially around the z-axis which cause no net-inclination change can be caused by cycles of freeze-thaw. In this work, we identified the individual events using a new custom-written algorithm. Each movement event predicted by the algorithm was checked manually by looking at plots of the inclination, checking for the above indicators to find the events belonging to the first two groups.

The algorithm has four hyperparameters (referred to as n_1-n_4). For each point in time with a measurement (t_n), the algorithm calculates **1.** The standard deviation (σ_{long}) of the n_1 measurements before t_n, and **2.** The standard deviation (σ_{short}) of the n_2 measurements around t_n. A potential event was considered to have started when the condition $\sigma_{short} > n_3 \times \sigma_{long}$ was met. A potential event was considered to have ended when $\sigma_{short} < n_4 \times \sigma_{long\_start}$, where σ_{long_start} is the σ_{long} of the t_n when the event started. Here n_1 and n_2 are real positive integers with $n_1 > n_2$, and n_3 and n_4 are real positive numbers with $n_3 \geq n_4$. The best values for n1-n4 were found by running the algorithm for a range of values and identifying for which combination of values the algorithm best predicted manually identified events which occurred between sensor installation and 23 May 2023; in this dataset all environmental conditions occur. Furthermore, to identify the performance of the estimator, we used 3-fold cross-validation.

The best prediction is defined as the prediction that produced the lowest value for the following cost function:

$$C = \sum_{i=1}^{N} \delta_i^{mismatch} + 216 \sum_{j=1}^{E} \delta_j^{missed} \quad (1)$$

where N is the number of measurements and E are the number of manually identified events and $\delta_i^{mismatch}$ and δ_j^{missed} are defined as:

$$\delta_i^{mismatch} = \begin{cases} 0 \text{ if } p_i = m_i \\ 1 \text{ if } p_i \neq m_i \end{cases} \quad (2)$$

where p_i represents the prediction by the algorithm at each time point t_i (0 if not in an event, or 1 if in an event) and m_i represents if the same point is considered part of an event (0 if no, or 1 if yes) by the manual identification;

$$\delta_j^{missed} = \begin{cases} 1 \text{ if } \sum_{k=1}^{N_j} p_k = 0 \\ 0 \text{ otherwise} \end{cases} \quad (3)$$

where N_j is the number of points in the manually identified event j, and p_k are the predictions (0 if not in an event, or 1 if in an event) by the algorithm of the time points in the manually identified event.

Essentially, the first part of C punishes the algorithm for misidentifying a point as being in an event or not. The second part of C punishes the algorithm even more if no points in a manually identified event are identified as being part of an event (i.e. the event is missed by the algorithm). The value 216 represents a duration of 3 days (as there are 216 measurements in 3 days when they are spaced out by 20 min). This ensures that the algorithm is more likely to identify something as an event when it is not, than vice versa.

A manual check was performed to all identified events; found events that are not real events were removed from the selection. The manual check was performed by looking at a graph of the inclination around the x- and y-axes starting $3 \times n_1$ measurements before the start of the identified event until $3 \times n_1$ measurements after the identified event finished, with the duration of the identified event highlighted. An identified event was considered a real event when a significant and permanent inclination change was visible around at least one of the axes.

2.4. Timeseries analysis

In this study, we investigate the data obtained using the soil sensors between 17/11/2022 and 17/11/2023, e.g. a one year data set starting at the beginning of the winter period. One of the installed sensors had already been lost before the study period started (see also van Rooijen et al., 2023). For each site, a cumulative distribution function (CDF) for the movement events identified using the previously described algorithm was computed to identify when events occurred more frequently. The time periods with increased movement were compared to air temperature, precipitation intensity and water level or discharge timeseries to identify what the potential causes for events are.

Furthermore, to get an even better insight into the drivers of bank erosion, we calculated for each bank erosion event the time it occurred after several specific types of environmental events. The following environmental events were considered: increases in soil moisture larger than 0.1 % at the sensor location that moved, thawing of the soil (as measured by the air or soil temperature at the sensor location going from negative to positive) and precipitation events larger than 1 mm/h. These time lags were used to make a cumulative distribution function which we compared with the cumulative distribution function that would be obtained using the same procedure if all soil movement events were uniformly distributed throughout the investigated period. The time-lapse camera, installed at the Pulmankijoki River site, was used for visually confirming specific movement events and their possible driving agents.

3. Results

3.1. Seasonal air temperature and precipitation in relation to overall soil sensor parameter value changes

Measurements from representative sensors at each field location are shown in Figs. 3–5. These show that soil moisture increases after intense or frequent precipitation events followed by reductions towards stable levels and the diurnal soil temperature profile lagging several hours behind the air temperature. Furthermore, some clear movement events are visible, with movement being episodic in nature and more frequent in the Pulmankijoki fieldsite than the Oulankajoki and Vantaanjoki fieldsites. At the Pulmankijoki fieldsite movement events clearly cluster together in certain time periods. Finally, the spring flood occurred later in the year in the more Northern field sites, with two floods occurring at the Vantaanjoki field site, the first one in still in winter.

During the freezing and thawing of the soil a very clear different pattern is evident (Figs. 3–5). When air temperatures first drop below zero, soil temperatures reduce and then remain stable at 0 °C losing its diurnal pattern. A strong decrease in soil moisture, often to zero can then be observed, from which point onwards soil temperatures can drop further. Measured soil temperatures while the soil is frozen generally are more stable and closer to the upper range of the air temperature range compared to the non-frozen period. The freezing and thawing can also cause diurnal patterns in soil moisture concentration in spring and autumn, with generally sharp increases and decreases in soil moisture. This soil moisture pattern is similar to that described by Wynn et al. (2008).

At the Pulmankijoki and Oulankajoki sites (Figs. 3 and 4), the soil remains frozen throughout the winter period, with a stable and low soil moisture concentration and soil temperatures below 0 °C. When air temperatures increase and the soil thaws a different pattern is visible: before soil temperatures reach 0 °C, soil moisture already shows a stark increase, often to values significantly higher than those before freezing of the soil. Only after soil moisture has reached peak value, soil temperatures increase to values above 0 °C.

At the Vantaanjoki site (Fig. 5), measured soil temperatures remained around 0 °C throughout the winter period, only occasionally deviating from this value. Soil moisture is high throughout winter (compared to the rest of the year), with only at some locations the clear drop in soil moisture associated with soil freezing, usually followed by an increase in soil moisture associated with thawing of the soil within a

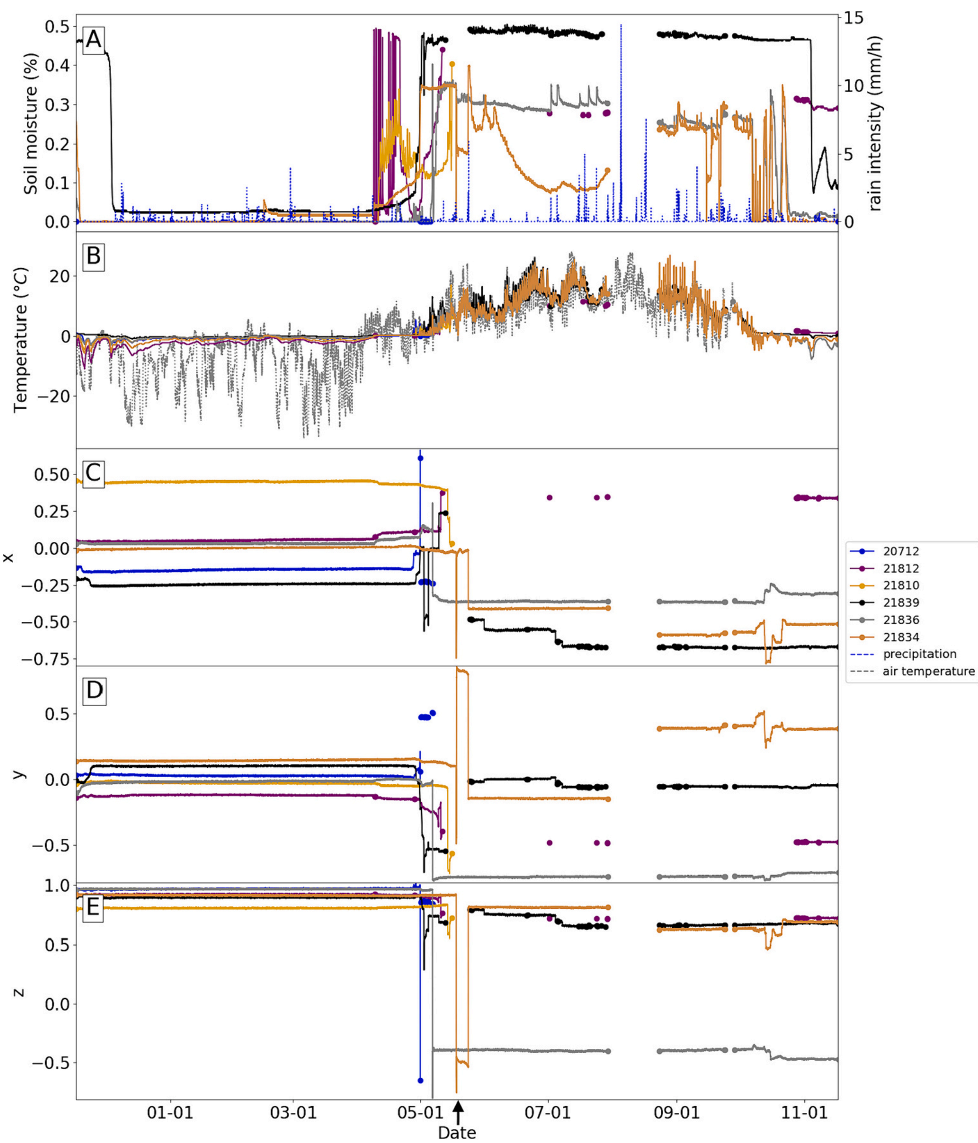

Fig. 3. Measurements at the Pulmankijoki field site for a few selected sensors. A soil moisture and rainfall intensity, **B** soil and air temperature, **C, D** and **E** the orientation around the x, y and z axes, respectively. The arrow indicates the timing of the spring flood.

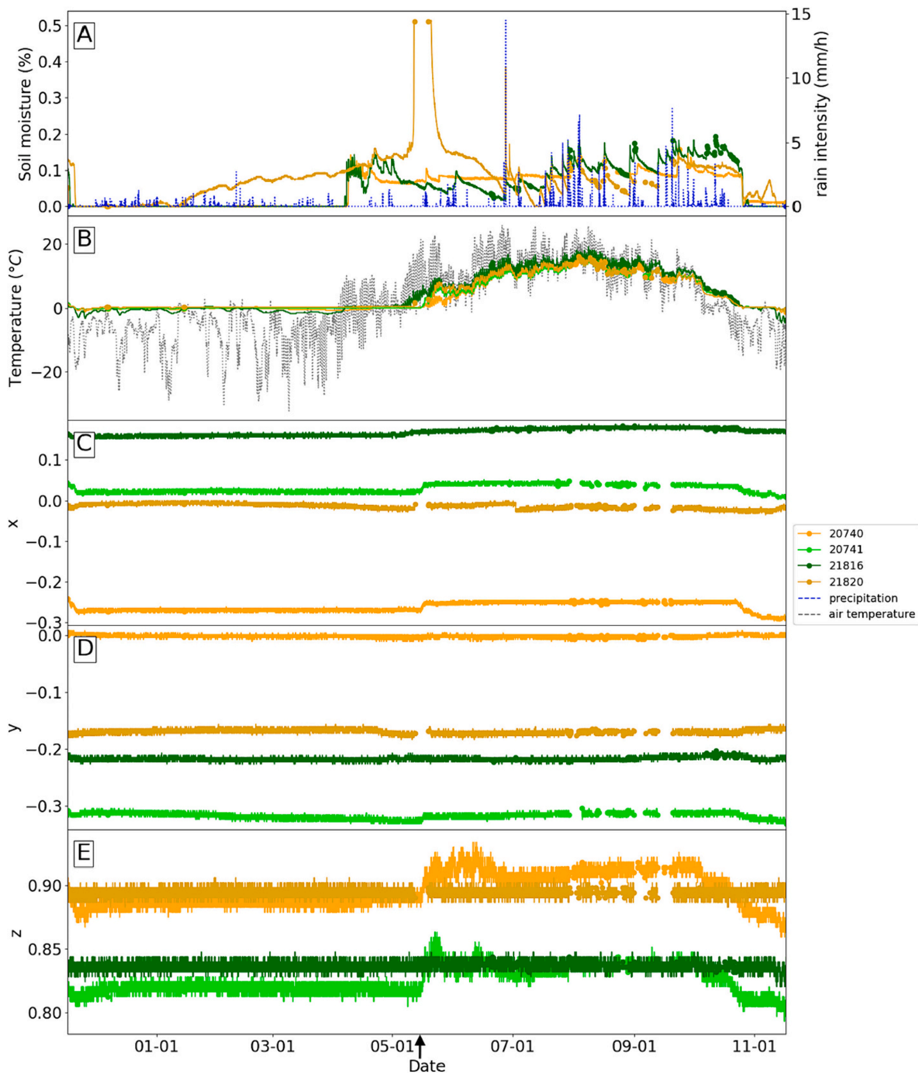

Fig. 4. Measurements at the Oulankajoki field site for a few selected sensors. **A** soil moisture and rainfall intensity, **B** soil and air temperature, **C**, **D** and **E** the orientation around the x, y and z axes, respectively. The arrow indicates the timing of the spring flood.

couple days.

3.2. Soil movement events and their physical drivers

During the investigated period several sensors were lost at the Pulmankijoki site. Sensor 20,714 became unstable about 1 day before the investigated period and continued to move until it was lost. The freezing of soil was already occurring at the time. The other two (20,712 and 21,810) were lost during the thawing period (May 2023) after becoming unstable in the beginning of April 2023 (Fig. 3). Both of these sensors had also moved shortly after the beginning of the investigation period. Sensor 20,713 had already been lost before the investigation period started. All the sensors that were lost, were located close to the waterline at the Pulmankijoki site.

Sensors that were not lost, moved considerably as well. Sensor 21,812 (close to water line) became unstable in the beginning of April 2023 and experienced several movement events until 11 May 2023, when the connection with it was temporarily lost (Fig. 3). Connection was re-established on 27 October 2023. The other sensors followed a similar pattern, with potential movement shortly after the initiation of the investigation period (21,839, far from water line) and becoming unstable in April 2023 (sensor 21,836; far from water line), then showing one or several movement events until the end of May (21,834, 21,836, 21,839), usually with at least one event close to the end of May which changed the sensors orientation more. More movement events then occurred in October (21,834, 21,836). Sensor 21,839 (close to water line) also measured some movement events during the summer period.

At the Oulankajoki and Vantaanjoki field sites, movement events were less frequent. At the Oulankajoki field site, sensors 20,740 and 20,741 show small movements shortly after the start of the investigation period, around 16 May and close to the end of October.

Besides these movement events, also movements only around the z-axis are sometimes occurring, which are diurnal in nature, mimicking the temperature regime (Fig. 6). These kinds of movements occur at all field sites, occurring in spring when soil temperatures rise above zero and in autumn when temperatures are close to zero.

The best values for n_1, n_2, n_3 and n_4 in the algorithm for automatic detection of movement events were found to be 90, 40, 1.4 and 1.4, respectively. Using these values the algorithm identified a total of 477 events, which after a manual check were reduced to 309 events. Fig. 7 shows that at the Pulmankijoki and Oulankajoki field sites a majority of events occurred just before and during the spring flood with some more during autumn and that especially few events occurred both during the winter and summer periods. At the Pulmankijoki field site, the sensors close to the water line detected 66 (33 %) events and the other sensors

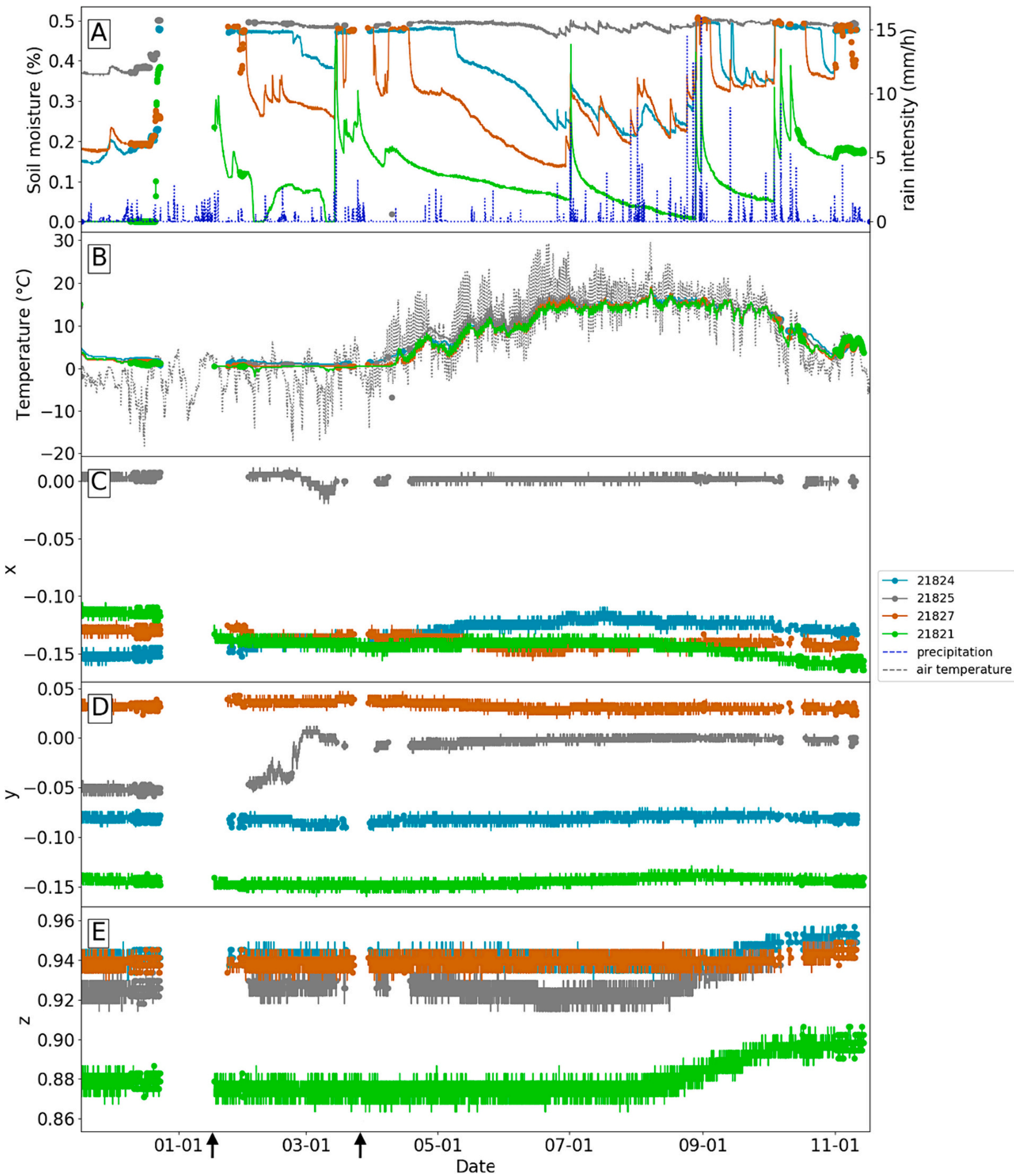

Fig. 5. Measurements at the Vantaanjoki field site for a few selected sensors. A soil moisture and rainfall intensity, **B** soil and air temperature, **C**, **D** and **E** the orientation around the x, y and z axes, respectively. The arrows indicate the timing of floods.

133 (67 %). This is close to the ratio of how the sensors are divided (36 % close to the water line), despite the fact that three sensors close to the water line were lost during the study.

The majority of the events occurred just before and during the spring flood at the Pulmankijoki and Oulankajoki field sites (Fig. 7A and B). Also during the autumn an increased amount of events occurred. At the Oulankajoki field site another short period in the middle of winter, when air temperatures were slightly above 0 °C during some days shows an increased frequency of soil movement events. At the Pulmankijoki field site, both the sensors located close to the waterline and those further away showed the same distribution of events in time, although close to the water line events were more frequent in spring, and further away from the waterline more in the autumn. At the Pulmankijoki site another slight increase in the frequency of events is evident in July (Fig. 7A), especially closer to the water line. No clear pattern in the distribution of events in time is evident at the Vantaanjoki field site and events seem to occur more or less uniformly in time (Fig. 7C).

At the Pulmankijoki River field site, the time between the soil moisture increasing and a soil movement event as well as the time between the soil temperature becoming positive and a soil movement event was shorter than when the soil movement events had been uniformly distributed (Fig. 8 A and B). The time between the air

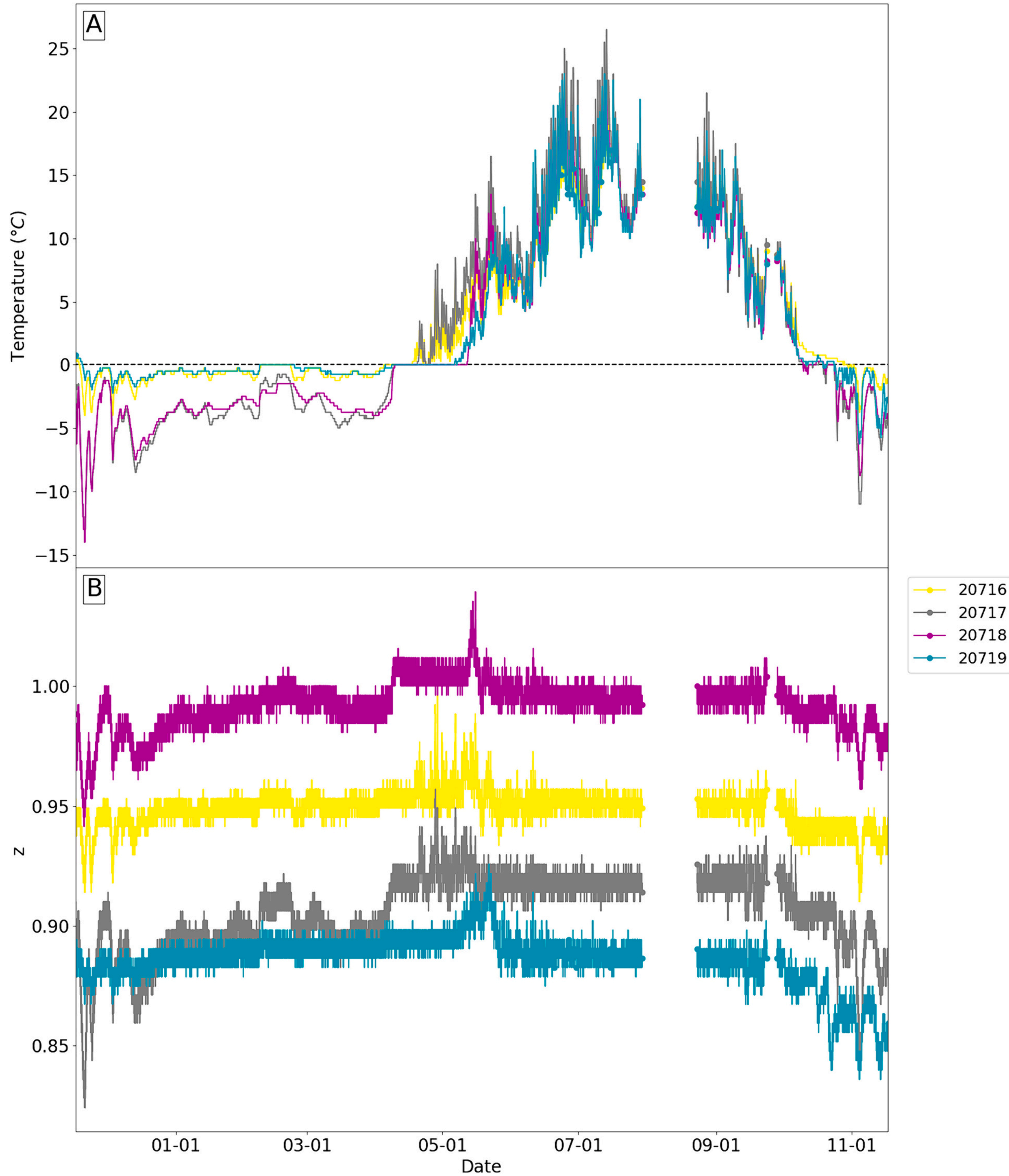

Fig. 6. Example of some sensors showing movement around the z-axis mimicking the temperature distribution. Panel **A**. shows the soil temperature measured by the sensor and panel **B**. the inclination around the z-axis.

temperature becoming positive and a soil movement event is short but rather similar to how these times would be when the soil movement events had been uniformly distributed. At the Oulankajoki field site the time between the air temperature becoming positive and a soil movement event is shorter than what would happen if movement events were uniformly distributed (Fig. 8E); the same is true to a lesser extent for a soil moisture increase (Fig. 8D). At the Vantaanjoki field site, the time between a soil moisture increase or the air or soil temperature becoming positive and a soil movement event are not shorter than if the movement events were uniformly distributed throughout the year (Figs. 8G and H). Many movement events seem to happen approximately 70 to 130 days after the soil temperature became positive at the Vantaanjoki fieldsite. For all field sites the time between a precipitation event and a soil moisture event are similar to what would be the case when movement events had been uniformly distributed in time (Fig. 8C, F and I).

3.3. *Time lapse camera imagery*

The time lapse imagery showed that during the spring flood at the Pulmankijoki fieldsite a large slab of soil slid into the river over the

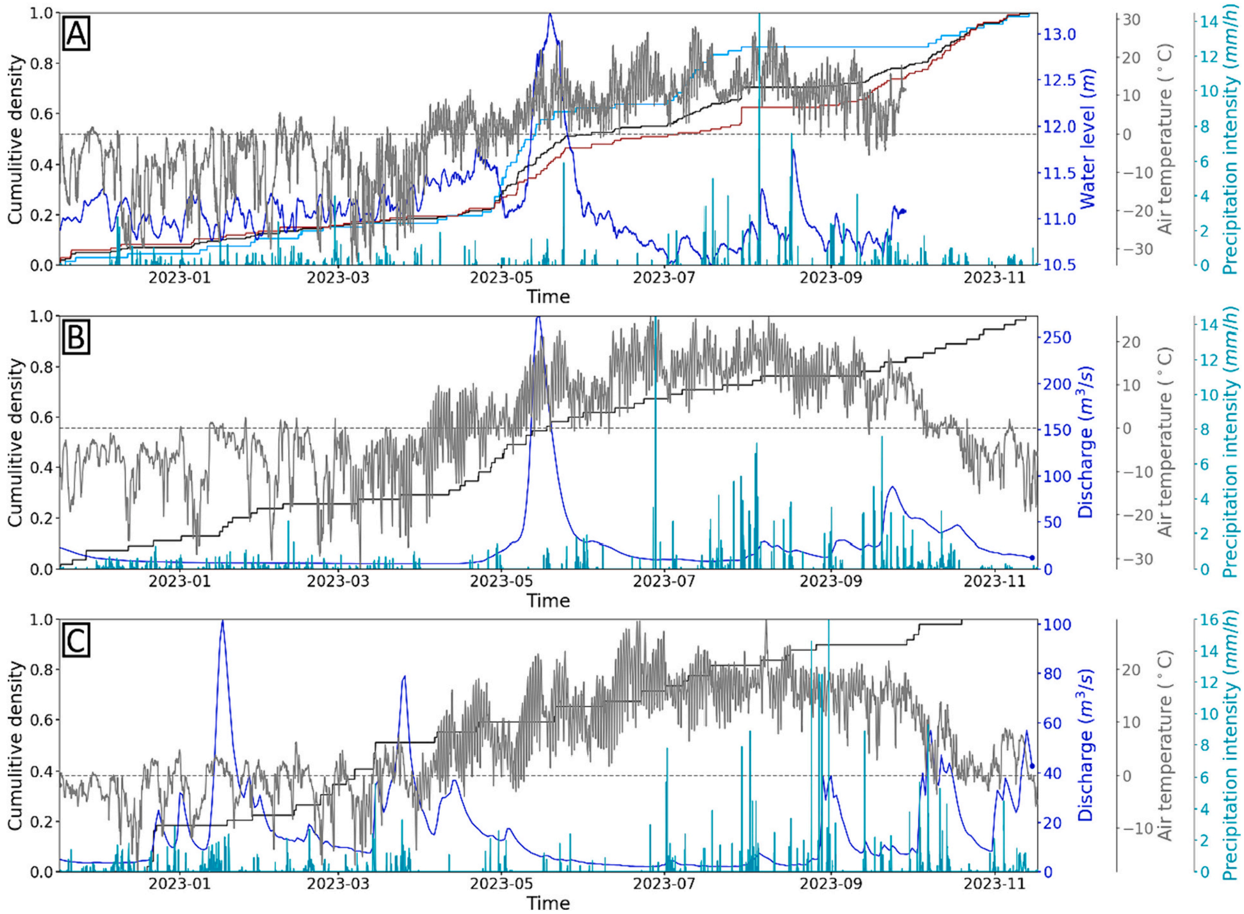

Fig. 7. Cumulative distribution functions (CDFs) for the soil movement events, and overview of environmental parameters for the Pulmankijoki (**A**), Oulankajoki (**B**) and Vantaanjoki (**C**) field sites. The soil movement events occurring around the x and y axes at each of the three field sites (black), shows when events occurred more frequently. For the Pulmankijoki River fieldsite, three CDFs are shown, one for the sensors located close to the water line (light blue), one for all other sensors (brown) and one for all installed sensors (black). The air temperature (grey), discharge/water level (blue) and precipitation intensity (cyan) at each field site are added for reference. (For interpretation of the references to colour in this figure legend, the reader is referred to the web version of this article.)

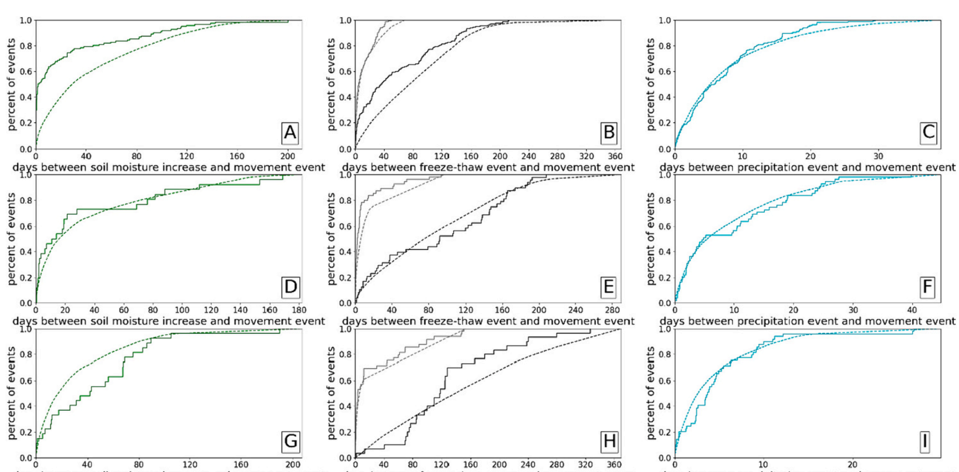

Fig. 8. Cumulative distribution functions of the time between a certain event and a soil movement event. From top to bottom the Pulmankijoki (**A-C**), Oulankajoki (**D-F**) and Vantaanjoki (**G-I**) field sites. From left to right the time between a sudden soil moisture increase (green; **A**, **D** & **G**), air temperature going from negative to positive (grey; **B**, **E** & **H**), soil temperature going from negative to positive (black; **B**, **E** & **H**) and a precipitation event larger than 1 mm/h (cyan; **C**, **F** & **I**). The dashed lines indicate what the distribution would look like if the soil movement events had been uniformly distributed throughout the year. (For interpretation of the references to colour in this figure legend, the reader is referred to the web version of this article.)

Fig. 9. Six photos taken during the spring flood at the Pulmankijoki field site, showing the erosion of a large slab of soil. Photos are taken on **A**. 13 May 2023, B. 14 May 2023, C. 15 May 2023, D. 16 May 2023, E. 17 May 2023 and F. 18 May 2023. All photos were taken at 22:41. A timelapse video of all pictures during the spring flood can be found in the supplementary material. The white lines indicate the highest and lowest flow identified on all images (17/11/2022–19/09/2023), with a water level difference of approximately 2.7 m.

course of several days (Fig. 9). The first signs of the erosion of the slab could be seen at the beginning of 13 May 2023, when a horizontal tear formed in the soil surface, which gradually widened over time. A large wedge of soil then slid down over a smooth surface over the course of several days, while the lower parts of the wedge continuously fell down into the river.

In addition, the photos also show that reindeer frequently visit the Pulmankijoki fieldsite and also wander onto the river bank, walking via multiple routes (Fig. 10). Considering the bank has a slope close to the angle of repose, we hypothesize that the trampling of reindeer could initiate soil movement. Considering all photos throughout the year (Fig. 11), shows that reindeer are most often in the area and on the river bank in July. For this quick analysis photos during the night were not considered, though during the darker periods of the year footprints in the snow could be used as indicators of reindeer presence (snow was present in the period November–April).

4. Discussion

4.1. Drivers of the measured spatiotemporal distributions of bank erosion

At the Pulmankijoki field site more movement events occurred than at the other two, most likely due to the lower extent of vegetation at this location (vegetation cover seen from Fig. 1). The roots of plants can reinforce the soil (Hubble et al., 2010), making all of the most prominent erosive processes less likely to occur.

Floods generally have received much scientific attention for their erosive effects on river banks, also in cold-climate regions (e.g. Nanson and Hickin, 1986; Densmore and Karle, 2009; Yao et al., 2011; Alexeevsky et al., 2013; Lotsari et al., 2020). Spring floods have received much attention as they are generally the largest fluvial events in these regions. Fig. 7 shows that around the timing of the spring flood (the peak in discharge) a disproportionally large number of soil movement events occurred. Furthermore Fig. 9 showed that the largest soil erosion event, that likely supplied the largest amount of sediments to the river occurred during the spring flood.

However, already before the spring flood started, the soil started moving (Fig. 7), indicating that the spring flood itself is not the main driver of these movement events. At this time the air temperatures were regularly above 0°C and also the soil thawed (Figs. 3–5). This insinuates that the thawing of the soil is the actual driver of the soil movement. The short times between temperatures becoming positive and a soil movement event, as well as the short time between a soil moisture increase and a soil movement event (Fig. 8), both also insinuate that thawing of the soil is an important driver for soil movement at least at the Pulmankijoki and Oulankajoki field sites, as they are both indicators of the thawing of soil. Previous research at the Pulmankijoki fieldsite (Lotsari et al., 2020) found that soil erosion began during the downramping

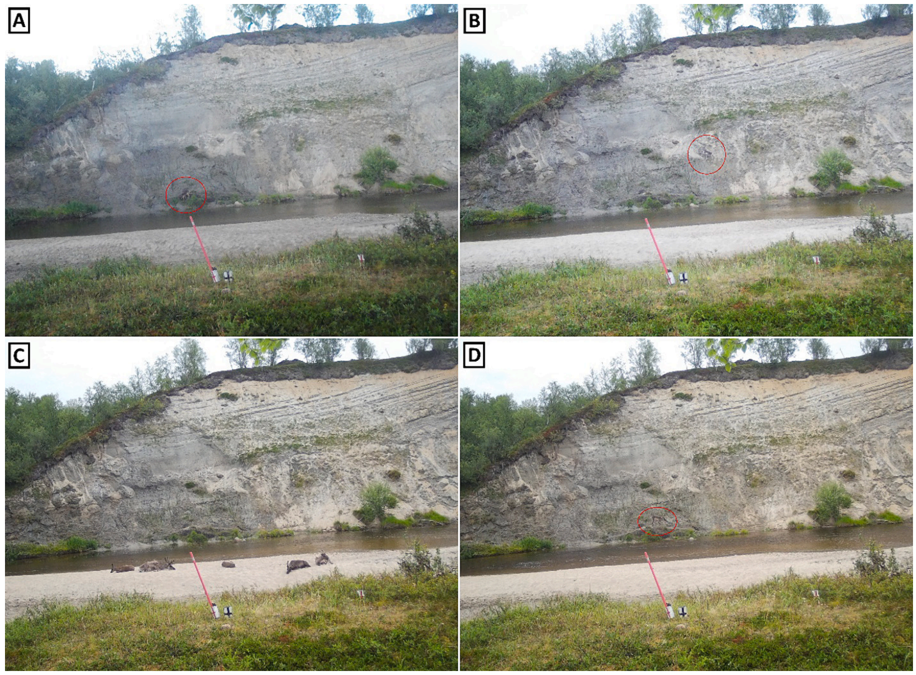

Fig. 10. Examples of photos showing reindeer at the Pulmankijoki field site. In case reindeer are on the bank, a red oval has been added for ease of spotting. Photos were taken on **A**. 17/07/2023 23:58, **B**. 25/07/2023 21:58, **C**. 27/07/2023 09:58 and **D**. 31/07/2023 13:58. (For interpretation of the references to colour in this figure legend, the reader is referred to the web version of this article.)

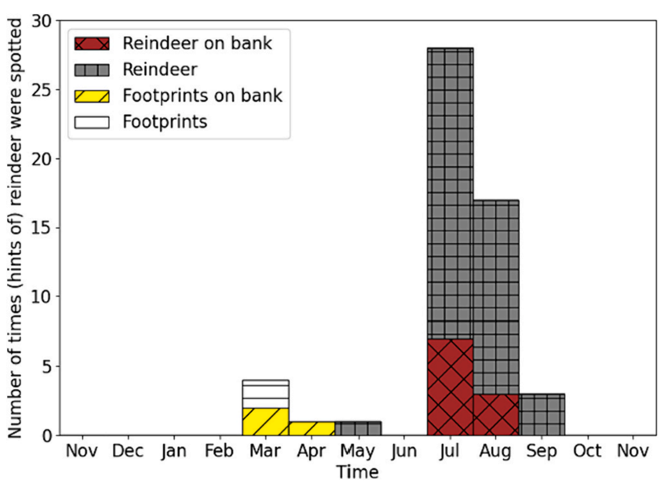

Fig. 11. Overview of when (hints of) reindeer were spotted on the camera. A division is made between reindeer seen on the bank itself, on the photo or if footprints of reindeer were seen on the photo in the snow, either on the bank or elsewhere on the photo.

phase of the spring flood (thus later than found in this work), and was most mostly associated with the timing that the soil thawed.

Furthermore, for many sensors soil movement around the z-axis is evident that mimics the soil temperature changes during the freezing and thawing periods (Fig. 6). This likely represents frost heave. These observations show that more than the spring flood, the thawing of the soil causes most of the soil movement events, and therefore bank erosion. The spring flood itself is thus likely not a strong erosional event (for the river banks), but rather transports already eroded material downstream, as has been suggested before by Lawler (1986). The large soil erosion event identified on the time lapse camera (Fig. 9) may also be due to freeze-thaw, even though it occurred during the spring flood. A similar event was described by Augustowski and Kukulak (2021) who found that a wedge of thawed soil could slide down a river bank over a layer of still frozen soil, with the bottom parts of the wedge breaking off and falling down.

The influence of freeze-thaw is largest at the Pulmankijoki field site, and least at the Vantaanjoki field site (Fig. 8), and thus increases with latitude. Fig. 8 shows that at the Oulankajoki field site, soil movements occur shortly after air temperatures became positive, while at the Pulmankijoki field site soil movements were more strongly linked to the soil temperature becoming positive. This could indicate that the freezing of the soil that causes soil movements, is more deep in the Pulmankijoki field site.

Furthermore, at the Pulmankijoki field site, the soil movements close to the water line were more concentrated in the spring and less in the autumn. Gardiner (1983) already found that erosion on the top and middle of a bank was dominated by freeze-thaw processes while at the bottom of the bank by fluvial erosion. Erosion caused by the spring flood could thus cause this distribution. However, although Yumoto et al. (2006) found that freeze-thaw uniformly affects a river bank, the additional water available close to the water line might also cause more water to freeze there (Branson et al., 1996; Matsuoka, 1996), causing more erosion upon thawing in spring.

Finally, at the Pulmankijoki field site an additional peak of soil movement could be found in July, which none of the considered environmental conditions could explain. This period was however unique due to the number of reindeer visiting the site (Fig. 11). Reindeer may thus be a disturbance causing river bank erosion, besides their recorded effects on vegetation (Evans, 1996; Bernes et al., 2015; Stark et al., 2022). A likely way they could do this is walking on part of the bank surface that is already close to instability. This could cause some of the soil to slide down, not too dissimilar to how grazing animals can cause erosion along river banks (Evans, 1996, 1998). This would also explain why in August, when reindeer are still active in the area, soil movement is less. At that point in time, most of the areas on a reindeer's potential path and which are close to instability have then already failed. Why reindeer cause soil movement more close to the water line, could be because these areas were left more unstable or because reindeer visit these areas more frequently. The data presented here are a strong indicator that reindeer may contribute to river bank erosion but does not give conclusive evidence and more research is required to prove or disprove this hypothesis.

4.2. Potential sources of errors

Due to various reasons, data from the sensors have gaps. At the Vantaanjoki River fieldsite, there is a data gap close to the beginning of the study period due to a battery failure of the base station which uploads the data of the wireless sensors. A similar issue occurred at the Pulmankijoki site in August. Furthermore, data gaps exist during the two spring floods that occurred in 2023, likely due to sensors temporarily being below the water level, limiting the radio signal transmitting the data. This also occurred at two sensor locations in the Oulankajoki field site. If the orientation of the sensor changed during the data gap, it could be inferred that a movement event had occurred, of which the timing could not be accurately assessed. In the analyses these movement events were considered to have lasted the entire data gap.

We found that soil movement events are more likely caused by freeze-thaw than spring floods. However, the fact that the timing of thawing and the spring flood are largely overlapping makes this analysis difficult. Since the spring flood is caused by water from melting snow, it is inextricably linked to the temperature regime. Therefore, by the very nature of the processes, it is impossible to study these two processes separately in the field. The statistical analyses show a clear pattern that supports that freeze-thaw is the dominant driver of river bank erosion, especially in the more Northern field sites.

Furthermore, the dataset obtained in this study may not be representative for most years, as it was gathered during an El Niño year. This is especially the case because the investigated phenomena are strongly dependent on temperatures, and it has been suggested that El Niño can cause lower temperatures in the investigated region (Ineson and Scaife, 2009). A longer investigation period may thus yield more representative results for normal years and shed light on the year to year variability in the temporal distribution of river bank erosion. Notwithstanding, the data from this study already did allow us to link river bank erosion events to environmental conditions and understand the spatiotemporal distribution of these events in a specific year.

In this research we investigated the frequency of soil movement events in river banks. However, not every movement event will necessarily transport the same amount of sediment towards the river and some events may thus be more important than others in shaping landscapes and supplying sediments to rivers. From our dataset, it is impossible to say with certainty which events transport more sediments. However, events that cause a larger change in sensor orientation are likely to move more soil. At the Pulmankijoki field site, these large events occur mostly during the spring flood and most of the sensors affected by the large events are located close to the water line, though not all. Especially the movement event shown in Fig. 9 might have caused many of the identified soil movement events and supplied the majority of sediments to the river.

Large soil movement events may also have significantly moved the sensors that were buried in the river bank. The sensors only register their orientation, not their location. The exact location of the sensors has thus become unknown. Sensors that are further away from the waterline may thus have moved down towards the waterline without that becoming evident. A similar movement event at a sensor location close to the waterline could move that sensor into the river where it can be washed away, leading to sensor loss.

The field sites are very different with regards to their vegetative conditions, which likely influenced the erosion processes between the field sites. However, the focus of this paper was not in vegetation, and we are not able to use it as explanatory factor yet. The topic of vegetation differences between sites and their relation to erosion will be a topic of a future study.

4.3. Significance for the future

The river banks studied in this work are representative of conditions in the cold climate category of the Köppen-Geiger classification, which is common in the Northern hemisphere (Fig. 2). Furthermore, their geomorphological characteristics and soils are representative for the majority of Fennoscandinavia, northwestern Russia and northern and eastern Canada (c.f. Bouysse et al., 2014). The studied river reaches are thus representative for many sites in the cold-climate region and we can expect that for the majority of these sites, most soil movement events occur during spring and autumn due to freezing and thawing of the soil, except along the warmer margins of this climatic zone. Permafrost was not considered in this study as it is not present in river banks in Fennoscandinavia, it only occurs in mountainous areas and sporadically elsewhere (see Brown et al., 1997; Verdonen et al., 2023).

However, it is likely that the temporal and spatial distributions of river bank erosion as measured will change in the future due to climate change, at the investigated bank sites and at similar sites. The frequency of freeze-thawing cycles is expected to change in Finland (Rasmus et al., 2020) and therefore it is also likely that the temperature regime in the soil is affected. The Vantaanjoki field site where complete freezing of the soil is already only occurring a few times per year, may not see any soil freezing (at sensor depth) anymore in the future. The effect of freeze-thaw in the south of Finland would then thus be limited to shallow freezing. At the Oulankajoki and Pulmankijoki sites the soil will likely be frozen for a shorter duration. As a result, the timing of the freezing and thawing of soil and the accompanying soil movement would shift (freezing later in the year, thawing earlier).

In this work we hypothesized that reindeer could play a role in eroding the bank at the Pulmankijoki field site, specifically in July. If this is indeed the case, the ways that reindeer migration patterns shift due to climate change, which is a complicated matter (e.g. Mallory and Boyce, 2018), can also impact the temporal distribution of bank erosion at this field site.

To better understand how bank erosion would change in both time and space under climate change-driven future conditions, modelling of river banks and their processes is required. To the authors knowledge, currently no models are available to model the freezing and thawing of soil at river banks. New modelling tools should thus be developed to improve our understanding of river bank erosion in cold climate environments. Such models will never be able to predict all bank erosion events, since the influence and timing of biological factors, such as reindeer or even humans, will be impossible to predict with high accuracy.

5. Conclusions

We obtained a one-year data set of river bank movement events covering all seasons and environmental conditions in three different field sites and used it to conduct statistical analyses to identify the temporal and spatial distributions of river bank erosion in cold-climate regions. The data insinuates that the freezing and thawing of the soil is the main driver of bank movement, with bank movement occurring most frequently during spring when soil thaws and secondarily in autumn when soil freezes. The spring flood occurring around the same time when soil thaws is likely of less importance in the investigated sites. Surprisingly, at one field site reindeer also seemed to be an driver of soil movement.

The freezing and thawing, as well as the accompanying soil movement is most pronounced in the more Northern field sites. At the Southernmost field site, little effect of the freezing and thawing of soil on the temporal soil movement distribution was identified.

On a smaller scale, the spatial distribution of soil movement at one bank site is less varied. The temporal distribution as well as the number of soil movement events close to the water line is very similar to those further up the river bank.

This research used a new type of dataset of soil temperature, moisture and movement never used before. This unique dataset allowed us to identify individual soil movement events and helps to better understand river bank erosion and by extension fluvial systems in cold-climates.

Supplementary data to this article can be found online at https://doi.org/10.1016/j.geomorph.2024.109140.

CRediT authorship contribution statement

Erik van Rooijen: Writing – review & editing, Writing – original draft, Visualization, Validation, Methodology, Investigation, Formal analysis, Data curation, Conceptualization. **Eliisa Lotsari:** Writing – review & editing, Supervision, Resources, Funding acquisition, Data curation, Conceptualization.

Declaration of competing interest

The authors declare that they have no known competing financial interests or personal relationships that could have appeared to influence the work reported in this paper.

Data availability

Data will be made available on request.

Acknowledgements

We would like to thank the Research Council of Finland for financially supporting this work (DefrostingRivers: 338480; HYDRO-RDI-Network: 337394; Digital Waters [DIWA] Flagship; 359248). In addition, the work was funded by the European Union – NextGenerationEU Recovery instrument (RRF) through Research Council of Finland projects Hydro RI Platform (346167) and Green-Digi-Basin (347703). Also funding was received from MVTT (Maa- ja vesitekniikan tuki ry: "The effects of changing bank erosion on river systems – study based on new measurement and modelling approaches", grant number 46475). Furthermore, we would like to thank MSc Tuure Takala (Aalto University), MSc Juha-Matti Välimäki (Aalto University) for aiding in the data collection throughout the observation period, Dr. Omid Saberi (Aalto University) and Miiro Jääskeläinen (Soilscout company) for helping with changing bases stations and other sensors in November 2022, and Dr. Mikel Calle Navarro (University of Turku) for helping with the issue with base station power supply at Pulmankijoki River in August 2023.

References

Alexeevsky, N.I., Chalov, R.S., Berkovich, K.M., Chalov, S.R., 2013. Channel changes in largest Russian rivers: natural and anthropogenic effects. Int. J. River Basin Manag. 11 (2), 175–191. https://doi.org/10.1080/15715124.2013.814660.

Asahi, K., Shimizu, Y., Nelson, J., Parker, G., 2013. Numerical simulation of river meandering with self-evolving banks. J. Geophys. Res. Earth 118 (4), 2208–2229. https://doi.org/10.1002/jgrf.20150.

Augustowski, K., Kukulak, J., 2021. The role of frost processes in the retreat of River Banks. Water 13 (13), 1812. https://doi.org/10.3390/w13131812.

Bernes, C., Bråthen, K.A., Forbes, B.C., Speed, J.D., Moen, J., 2015. What are the impacts of reindeer/caribou (Rangifer tarandus L.) on arctic and alpine vegetation? A systematic review. Environ. Evid. 4, 1–26. https://doi.org/10.1186/s13750-014-0030-3.

Bouysse, et al., 2014. Geological Map of the World at 1:35 M, revised issue 3rd edition. *CCGM-CGMW*. ISBN: 978-2-917310-24-3.

Branson, J., Lawler, D.M., Glen, J.W., 1996. Sediment inclusion events during needle ice growth: a laboratory investigation of the role of soil moisture and temperature fluctuations. Water Resour. Res. 32 (2), 459–466. https://doi.org/10.1029/95WR03400.

Brown, J., Ferrians, O.J., Heginbottom, J.A., Melkinov, E.S., 1997. Circum-Arctic Map of Permafrost and Ground-Ice Conditions. U.S. Geological Survey. https://doi.org/10.3133/cp45.

Chassiot, L., Lajeunesse, P., Bernier, J.F., 2020. Riverbank erosion in cold environments: Review and outlook. Earth Sci. Rev. 207, 103231 https://doi.org/10.1016/j.earscirev.2020.103231.

Couper, P.R., Maddock, I.P., 2001. Subaerial river bank erosion processes and their interaction with other bank erosion mechanisms on the River Arrow, Warwickshire, UK. Earth Surface Processes and Landforms: The Journal of the British Geomorphological Research Group 26 (6), 631–646. https://doi.org/10.1002/esp.212.

Darby, S.E., Rinaldi, M., Dapporto, S., 2007. Coupled simulations of fluvial erosion and mass wasting for cohesive river banks. J. Geophys. Res. Earth 112 (F3). https://doi.org/10.1029/2006JF000722.

Densmore, R.V., Karle, K.F., 2009. Flood effects on an alaskan stream restoration project: the value of long-term monitoring 1. JAWRA Journal of the American Water Resources Association 45 (6), 1424–1433. https://doi.org/10.1111/j.1752-1688.2009.00373.x.

Duró, G., Crosato, A., Kleinhans, M.G., Roelvink, D., Uijttewaal, W.S.J., 2020. Bank erosion processes in regulated navigable rivers. J. Geophys. Res. Earth 125 (7), e2019JF005441. https://doi.org/10.1029/2019JF005441.

Easson, G., Yarbrough, L.D., 2002. The effects of riparian vegetation on bank stability. Environ. Eng. Geosci. 8 (4), 247–260. https://doi.org/10.2113/8.4.247.

Evans, R., 1996. Some impacts of overgrazing by reindeer in Finnmark, Norway. Rangifer 16 (1), 3–19. https://doi.org/10.7557/2.16.1.1177.

Evans, R., 1998. The erosional impacts of grazing animals. Prog. Phys. Geogr. 22 (2), 251–268. https://doi.org/10.1177/030913339802200206.

Fox, G.A., Wilson, G.V., Simon, A., Langendoen, E.J., Akay, O., Fuchs, J.W., 2007. Measuring streambank erosion due to ground water seepage: correlation to bank pore water pressure, precipitation and stream stage. Earth Surface Processes and Landforms: The Journal of the British Geomorphological Research Group 32 (10), 1558–1573. https://doi.org/10.1002/esp.1490.

Frings, R.M., Gehres, N., Promny, M., Middelkoop, H., Schüttrumpf, H., Vollmer, S., 2014. Today's sediment budget of the Rhine River channel, focusing on the Upper Rhine Graben and Rhenish Massif. Geomorphology 204, 573–587. https://doi.org/10.1016/j.geomorph.2013.08.035.

Fuller, I.C., Marden, M., 2010. Rapid channel response to variability in sediment supply: cutting and filling of the Tarndale Fan, Waipaoa catchment, New Zealand. Mar. Geol. 270 (1–4), 45–54. https://doi.org/10.1016/j.margeo.2009.10.004.

Gardiner, T., 1983. Some factors promoting channel bank erosion, River Lagan, County Down. J. Earth Sci. 231–239. URL: https://www.jstor.org/stable/30002167.

Gatto, L.W., 1995. Soil Freeze-Thaw Effects on Bank Erodibility and Stability. Special Report 95-24. US Army Corps of Engineers Cold Regions Research and Engineering Laboratory, Hanover, NH. URL: https://hdl.handle.net/11681/12148.

Hagerty, D.J., 1991. Piping/sapping erosion. I: basic considerations. J. Hydraul. Eng. 117 (8), 991–1008. https://doi.org/10.1061/(ASCE)0733-9429(1991)117:8(991).

Hubble, T.C.T., Docker, B.B., Rutherfurd, I.D., 2010. The role of riparian trees in maintaining riverbank stability: a review of Australian experience and practice. Ecol. Eng. 36 (3), 292–304. https://doi.org/10.1016/j.ecoleng.2009.04.006.

Ineson, S., Scaife, A.A., 2009. The role of the stratosphere in the European climate response to El Niño. Nat. Geosci. 2 (1), 32–36. https://doi.org/10.1038/ngeo381.

IPCC, 2022. Climate Change 2022: impacts, adaptation, and vulnerability. In: Pörtner, H.-O., Roberts, D.C., Tignor, M., Poloczanska, E.S., Mintenbeck, K., Alegría, A., Craig, M., Langsdorf, S., Löschke, S., Möller, V., Okem, A., Rama, B. (Eds.), Contribution of Working Group II to the Sixth Assessment Report of the Intergovernmental Panel on Climate Change. Cambridge University Press, Cambridge, UK and New York, NY, USA. https://doi.org/10.1017/9781009325844, 3056 pp.

Kimiaghalam, N., Goharrokhi, M., Clark, S.P., Ahmari, H., 2015. A comprehensive fluvial geomorphology study of riverbank erosion on the Red River in Winnipeg, Manitoba, Canada. J. Hydrol. 529, 1488–1498. https://doi.org/10.1016/j.jhydrol.2015.08.033.

Kronvang, B., Grant, R., Laubel, A.L., 1997. Sediment and phosphorus export from a lowland catchment: quantification of sources. Water Air Soil Pollut. 99, 465–476. https://doi.org/10.1007/BF02406886.

Lawler, D.M., 1986. River bank erosion and the influence of frost: a statistical examination. Trans. Inst. Br. Geogr. 227-242 https://doi.org/10.2307/622008.

Lawler, D.M., 2005. The importance of high-resolution monitoring in erosion and deposition dynamics studies: examples from estuarine and fluvial systems. Geomorphology 64 (1–2), 1–23. https://doi.org/10.1016/j.geomorph.2004.04.005.

Lawler, D.M., 2008. Advances in the continuous monitoring of erosion and deposition dynamics: Developments and applications of the new PEEP-3T system. Geomorphology 93 (1–2), 17–39. https://doi.org/10.1016/j.geomorph.2006.12.016.

Lotsari, E., Vaaja, M., Flener, C., Kaartinen, H., Kukko, A., Kasvi, E., Alho, P., 2014. Annual bank and point bar morphodynamics of a meandering river determined by high-accuracy multitemporal laser scanning and flow data. Water Resour. Res. 50 (7), 5532–5559. https://doi.org/10.1002/2013WR014106.

Lotsari, E., Lind, L., Kämäri, M., 2019. Impacts of hydro-climatically varying years on ice growth and decay in a subarctic river. Water 11 (10), 2058. https://doi.org/10.3390/w11102058.

Lotsari, E., Hackney, C., Salmela, J., Kasvi, E., Kemp, J., Alho, P., Darby, S.E., 2020. Sub-arctic river bank dynamics and driving processes during the open-channel flow period. Earth Surf. Process. Landf. 45 (5), 1198–1216. https://doi.org/10.1002/esp.4796.

Mallory, C.D., Boyce, M.S., 2018. Observed and predicted effects of climate change on Arctic caribou and reindeer. Environ. Rev. 26 (1), 13–25. https://doi.org/10.1139/er-2017-0032.

Mansikkaniemi, H., Mäki, O.P., 1990. Paleochannels and recent changes in the Pulmankijoki valley, northern Lapland. Fennia-International Journal of Geography 168 (2), 137–152.

Matsuoka, N., 1996. Soil moisture variability in relation to diurnal frost heaving on Japanese high mountain slopes. Permafr. Periglac. Process. 7 (2), 139–151 doi: 10.1002/(SICI)1099-1530(199604)7:2<139::AID-PPP214>3.0.CO;2-V.

Nanson, G.C., Hickin, E.J., 1986. A statistical analysis of bank erosion and channel migration in western Canada. Geol. Soc. Am. Bull. 97 (4), 497–504 doi:10.1130/0016-7606(1986)97<497:ASAOBE>2.0.CO;2.
Neal, C.W.M., Anders, A.M., 2015. Suspended sediment supply dominated by bank erosion in a low-gradient agricultural watershed, Wildcat Slough, Fisher, Illinois, United States. J. Soil Water Conserv. 70 (3), 145–155. https://doi.org/10.2489/jswc.70.3.145.
Nones, M., 2019. Dealing with sediment transport in flood risk management. Acta Geophys. 67 (2), 677–685. https://doi.org/10.1007/s11600-019-00273-7.
Osman, A.M., Thorne, C.R., 1988. Riverbank stability analysis. I: Theory. J. Hydraul. Eng. 114 (2), 134–150. https://doi.org/10.1061/(ASCE)0733-9429(1988)114:2(134).
Paarlberg, A.J., Guerrero, M., Huthoff, F., Re, M., 2015. Optimizing dredge-and-dump activities for river navigability using a hydro-morphodynamic model. Water 7 (7), 3943–3962. https://doi.org/10.3390/w7073943.
Panin, A.V., Astakhov, V.I., Lotsari, E., Komatsu, G., Lang, J., Winsemann, J., 2020. Middle and Late Quaternary glacial lake-outburst floods, drainage diversions and reorganization of fluvial systems in northwestern Eurasia. Earth Sci. Rev. 201, 103069 https://doi.org/10.1016/j.earscirev.2019.103069.
Peel, M.C., Finlayson, B.L., McMahon, T.A., 2007. Updated world map of the Köppen-Geiger climate classification. Hydrol. Earth Syst. Sci. 11 (5), 1633–1644. https://doi.org/10.5194/hess-11-1633-2007.
Prosser, I.P., Hughes, A.O., Rutherfurd, I.D., 2000. Bank erosion of an incised upland channel by subaerial processes: Tasmania, Australia. Earth Surface Processes and Landforms: The Journal of the British Geomorphological Research Group 25 (10), 1085–1101 doi:10.1002/1096-9837(200009)25:10<1085::AID-ESP118>3.0.CO;2-K.
Rachelly, C., Mathers, K.L., Weber, C., Weitbrecht, V., Boes, R.M., Vetsch, D.F., 2021. How does sediment supply influence refugia availability in river widenings? J. Ecohydraul. 6 (2), 121–138. https://doi.org/10.1080/24705357.2020.1831415.
Rasmus, S., Turunen, M., Luomaranta, A., Kivinen, S., Jylhä, K., Räihä, J., 2020. Climate change and reindeer management in Finland: Co-analysis of practitioner knowledge and meteorological data for better adaptation. Sci. Total Environ. 710, 136229 https://doi.org/10.1016/j.scitotenv.2019.136229.
Rinaldi, M., Casagli, N., 1999. Stability of streambanks formed in partially saturated soils and effects of negative pore water pressures: the Sieve River (Italy). Geomorphology 26 (4), 253–277. https://doi.org/10.1016/S0169-555X(98)00069-5.
Rinaldi, M., Casagli, N., Dapporto, S., Gargini, A., 2004. Monitoring and modelling of pore water pressure changes and riverbank stability during flow events. Earth Surf. Process. Landf. 29 (2), 237–254. https://doi.org/10.1002/esp.1042.
Saarinen, N., Vastaranta, M., Vaaja, M., Lotsari, E., Jaakkola, A., Kukko, A., Alho, P., 2013. Area-based approach for mapping and monitoring riverine vegetation using mobile laser scanning. Remote Sens. 5 (10), 5285–5303. https://doi.org/10.3390/rs5105285.
Sekely, A.C., Mulla, D.J., Bauer, D.W., 2002. Streambank slumping and its contribution to the phosphorus and suspended sediment loads of the Blue Earth River, Minnesota. J. Soil Water Conserv. 57 (5), 243–250.
Soil Scout, 2022. Soil Scout Hydra User Manual. accessed 29.8.2022, available online: https://drive.google.com/file/d/0B4_CUFDRpzgXQnRPUGxTMGVBems/view?resourcekey=0-L-ho5Og10zjSyvXvPPFeHg.
Stark, S., Horstkotte, T., Kumpula, J., Olofsson, J., Tømmervik, H., Turunen, M., 2022. The ecosystem effects of reindeer (Rangifer tarandus) in northern Fennoscandia: past, present and future. Perspectives in Plant Ecology, Evolution and Systematics 125716. https://doi.org/10.1016/j.ppees.2022.125716.
Tiusanen, M.J., 2013. Soil scouts: Description and performance of single hop wireless underground sensor nodes. Ad Hoc Netw. 11 (5), 1610–1618. https://doi.org/10.1016/j.adhoc.2013.02.002.
van Rooijen, E., Siviglia, A., Vetsch, D.F., Boes, R.M., Vanzo, D., 2022. Quantifying fluvial habitat changes due to multiple subsequent floods in a braided alpine reach. Journal of Ecohydraulics 1-21. https://doi.org/10.1080/24705357.2022.2105755.
van Rooijen, E., Dietze, M., Lotsari, E., 2023. Employing novel wireless agricultural sensors for real-time monitoring of fluvial bank erosion. Earth Surf. Process. Landf. 48 (13), 2480–2499. https://doi.org/10.1002/esp.5640.
Vandermause, R., Harvey, M., Zevenbergen, L., Ettema, R., 2021. River-ice effects on bank erosion along the middle segment of the Susitna river, Alaska. Cold Reg. Sci. Technol. 185, 103239 https://doi.org/10.1016/j.coldregions.2021.103239.
Verdonen, M., Störmer, A., Lotsari, E., Korpelainen, P., Burkhard, B., Colpaert, A., Kumpula, T., 2023. Permafrost degradation at two monitored palsa mires in north-west Finland. Cryosphere 17 (5), 1803–1819. https://doi.org/10.5194/tc-17-1803-2023.
Waterinfo, 2023, *https://www.vesi.fi/karttapalvelu/*, accessed: 17 Nov. 2023.
Wynn, T.M., Henderson, M.B., Vaughan, D.H., 2008. Changes in streambank erodibility and critical shear stress due to subaerial processes along a headwater stream, southwestern Virginia, USA. Geomorphology 97 (3–4), 260–273. https://doi.org/10.1016/j.geomorph.2007.08.010.
Yao, Z., Ta, W., Jia, X., Xiao, J., 2011. Bank erosion and accretion along the Ningxia–Inner Mongolia reaches of the Yellow River from 1958 to 2008. Geomorphology 127 (1–2), 99–106. https://doi.org/10.1016/j.geomorph.2010.12.010.
Yumoto, M., Ogata, T., Matsuoka, N., Matsumoto, E., 2006. Riverbank freeze-thaw erosion along a small mountain stream, Nikko volcanic area, central Japan. Permafr. Periglac. Process. 17 (4), 325–339. https://doi.org/10.1002/ppp.569.